Supporting Information

Reduction of carbondioxide with mesoporous SnO_2 nanoparticles as active photocatalysts under visible light in Water

Arpita Hazra Chowdhury,[a] Anjan Das,[a] Sk Riyajuddin,[b] Kaushik Ghosh,[b] Sk. Manirul Islam*[a]

[a]Department of Chemistry, Kalyani University, Kalyani, West Bengal, 741235, India

[b]Institute of Nano Science and Technology, Mohali, 160062, India

Contents

Materials

$SnCl_4.5H_2O$, SDS and ammonium hydroxide (NH_4OH, 25% aqueous) were purchased from E-Merk, India. Deionized (DI) water wasused for all the experiments wherever needed. All the reactions were performed using oven-dried glassware under ambient atmosphere unless otherwise mentioned.

Instrumentation

Absorption spectroscopy: UV-Vis absorption spectrum of the catalyst was recorded on SHIMADZU, UV-2600 UV-Vis spectrometer with a standard 1 cm x 1 cm cuvette.

NMR Spectra: ^{1}H &^{13}C NMR Proton and ^{13}Carbon nuclear magnetic resonance spectra were recorded on a Bruker 400 MHz spectrometer. Chemical shifts for protons and ^{13}Carbon are reported in parts per million (ppm).

PXRD: The PXRD analysis was performed by using an X-raydiffractometer (BRUKER, Powder X-Ray eco D8 ADVANCE) equipped with Ni-filtered Cu K_α (λ= 0.15406 nm) radiation.

IR Spectra: The FTIR spectra of the materials were recorded from a Perkin-Elmer spectrophotometer (FT-IR 783) on KBr pellets.

SEM: FESEM images of the catalyst were acquired by using Scanning Electron Microscope (SEM) [JEOL JSM IT 300].

TEM: Transmission Electron Microscope (TEM) [JEOL JEM 2100] was used obtain the morphological information of the sample.

RAMAN: RAMAN spectrum of the catalyst was recorded by Confocal Raman Spectrometer [WITEC alpha 300 R].

TGA: The thermal stability of the COF material was analyzed by a Thermogravimetric Analyzer [SDT Q600 V20.9 Build 20].

BET: The N_2 adsorption-desorption analysis of TFPG-DAAQ COF sample was conducted by using a BET Surface Analyzer [QUANTACHROME ASIQCOV602-5].

Synthesis of Mesoporous TinOxide

The SnO_2 nanomaterial was prepared by using $SnCl_4.5H_2O$ and anionic surfactant SDS as Sn source and templating materials respectively. 3 mmol of SDS was first dissolved in 25 mL of water in ice-cold condition followed by addition of 9 mmol of $SnCl_4$ and the mixture was stirred for 1h. After that aqueous ammonium hydroxide solution was drop-wise added to the mixture in ice-cold condition maintaining the pH of the solution at ca. 4 followed by stirring for further 1h. Then the solution was aged for one day in ice-cold temperature at static condition. The white precipitate of tin oxide was then collected by centrifugation and washed it by using simple washing technique used in previously reported literatures [1,2] with DI water and acetone for multiple times to remove the template material as much as possible. People also used solvent extraction method for simple removal of template material [3]. However, we dried the synthesized material at 60 °C for 2 h.

Characterizations

PXRDAnalysis

The diffraction peaks present in the PXRD pattern (Figure S1)of the synthesized material clearly matched with the characteristic diffraction pattern of tin oxide material of JCPDS card no. 41-1445, having diffraction planes (110), (101), (211), and (112). Therefore, the wide-angle PXRD

analysis of the synthesized sample confirms the production of SnO_2 nanomaterial. The calculated crystallite sizes of the SnO_2 particles from the XRD data using Scherrer equation are very small (~3 nm).To understand the mesoporosity from PXRD analysis we have done the small angle PXRD study (Figure S2) of the synthesized SnO_2 sample where we have seen a single diffraction hump at low 2θ value which indicated the presence of meso-phases in the sample [3].

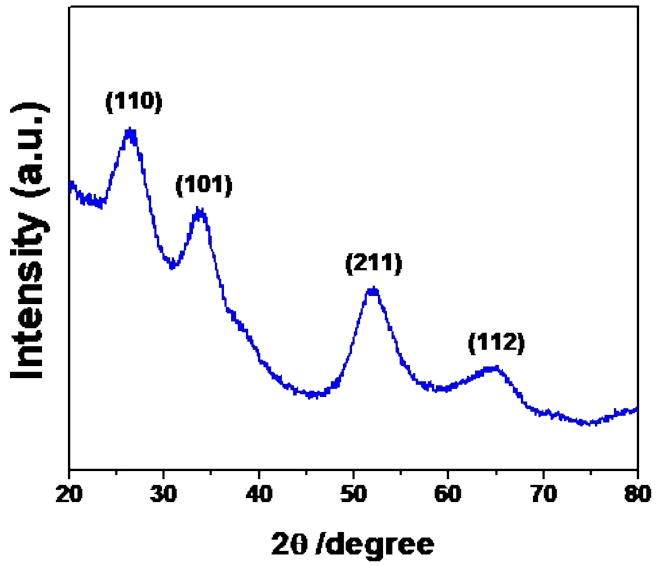

Figure S1. XRD pattern of the synthesized SnO_2 sample.

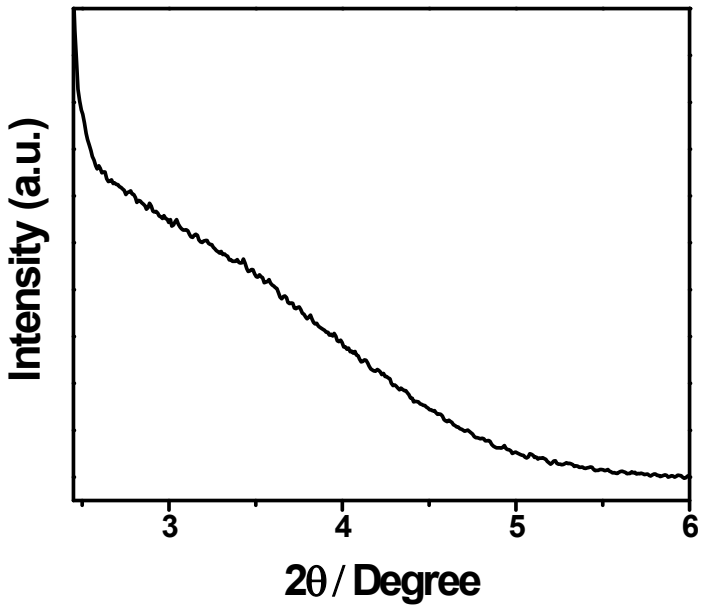

Figure S2. Small angle XRD patterns of SnO_2 material.

FTIR Analysis

The FTIR spectra (Figure S3) of the prepared sample indicated a broad intense band at 620 Cm^{-1} which corresponds to stretching of Sn-O bond [4] confirming the synthesis of SnO_2. The small peaks at 2861 and 2946 Cm^{-1} are due to C-H vibrations of the organic template SDS. Band at 3400 Cm^{-1} corresponds to the vibration mode of O-H bond of physisorbed water molecules [5].

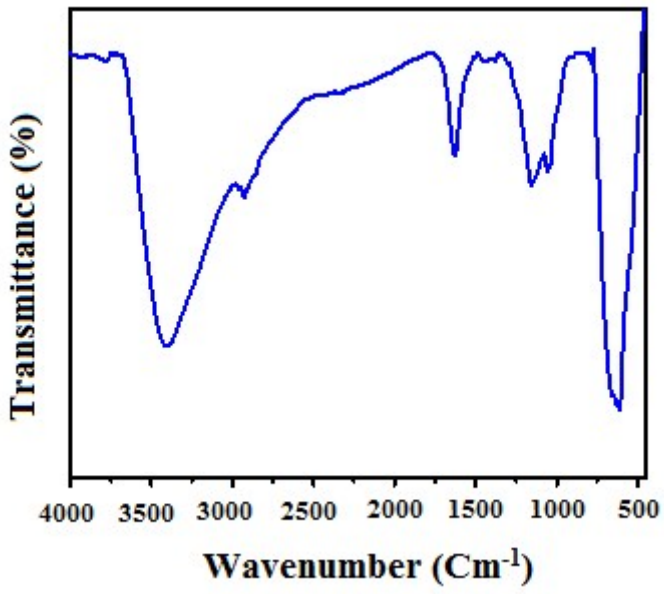

Figure S3. FTIR spectra of the SnO_2 sample.

RAMAN Analysis

The RAMAN spectra of the synthesized tin oxide material is shown in Figure S4. The peak at 470 Cm^{-1} corresponds to Eg mode originating from the mode of vibration of the oxide ions present in the SnO_2 nanomaterial [6]. The small peak at 772 Cm^{-1} corresponds to B2g mode originating from the Sn-O bond asymmetric stretching. The broad and strong band at 577 $Cm^{-1}$is

not generally observed in RAMAN spectra of SnO_2 material. The band arises due to the presence of very small size SnO_2 nanoparticles [7], which supports the XRD data.

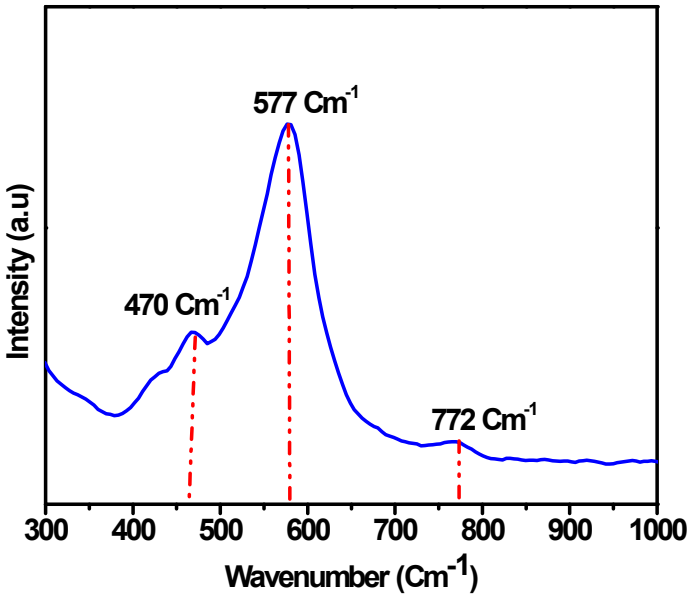

Figure S4. RAMAN spectra of the SnO_2 material.

UV-vis Analysis

UV-visspectroscopy (Figure S5)of the SnO_2 material was done to analyze its optical absorbance and band gap energy. The band gap energy was calculated by using the following equation [8]:

$E_g = (1239.8 / \lambda)$

Where, E_g = Energy band gap and

λ = Absorption edge wavelength (nm) in the spectrum

The $E_g$from this equation is calculated to be 2.92 eV which suggests the electron transfer occurs from valance band to conduction band under visible light irradiation.

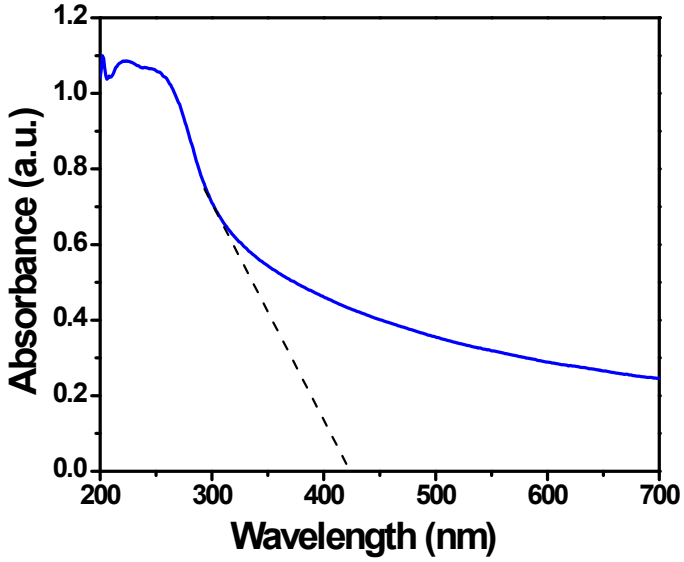

Figure S5.UV-vis spectra of the SnO_2 material.

N_2 adsorption–desorption Analysis

The N_2 adsorption–desorption isotherm of the SnO_2 material (Figure S6) signifies the existence of type IV isotherm with H3 hysteresis loop signifying the presence of slit like mesopores. The BJH PSD (pore size distribution) plot originating from the desorption datashowed that the sample has a narrow pore size distribution with pore diameter 3.6 nm which falls in the mesoporous region. The material has high BET surface area of 165.765 $m^2g^{-1}$and total pore volume of 0.21 cm^3g^{-1}.

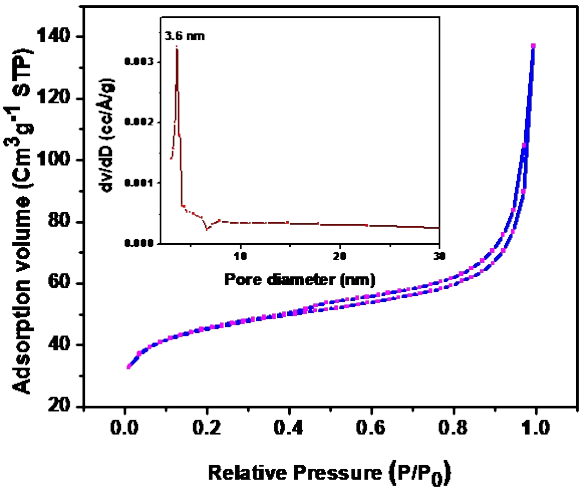

Figure S6. N_2 adsorption–desorption isotherm of the SnO_2 material at 77 K. Pore size distribution is shown in the inset.

Thermal Analysis

The thermal stability of the SnO_2 material was analyzed by thermogravimetric analysis of the sample. The thermogravimetric plot (Figure S7) of the material indicates that there are three step weight losses occurred. First step weight loss (~ 15%) upto 130^0C corresponds to desorption of surface adsorbed water. The further two step weight losses upto 460^0C correspond to the decomposition of small amount of organic templating agent. There was no further noticeable weight loss occurred above 460^0C temperature.

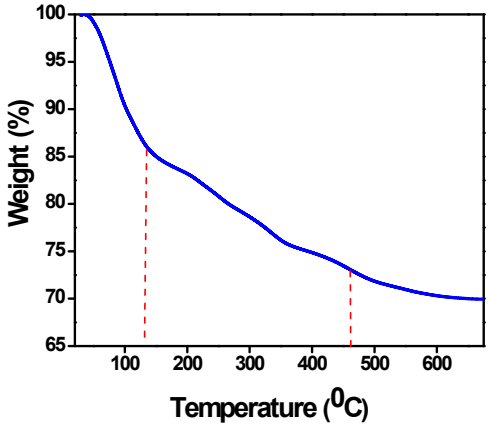

Figure S7. TGAplot of the SnO_2 material.

Microscopic Analysis

The morphological characteristics of the mesoporous SnO_2 material were studied by FESEM (Figure S8a, b) and TEM (Figure S9a, b) analysis. The FESEM images suggested that Small SnO_2nanoparticles are aggregated to for bigger size particles. The TEM image (Figure S9a) clearly indicates the existence of inter-particle porosity in the material. From the HRTEM image (Fig. S9b)of the SnO_2sample, the d-spacings are calculated 0.267nm and 0.34 nm which correspond to (101) and (110) planes of SnO_2respectively.The elemental composition (Sn and O) of the material is confirmed by the EDAX pattern (Figure S10).

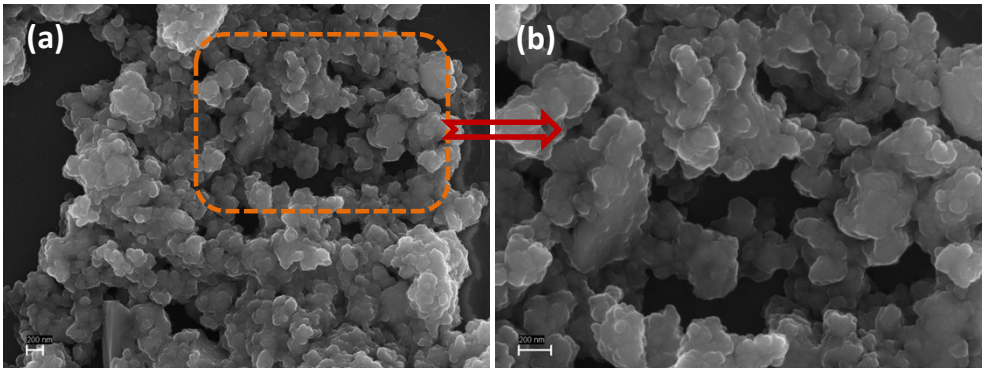

Figure S8.FE-SEM images of SnO_2 material at two different magnifications.

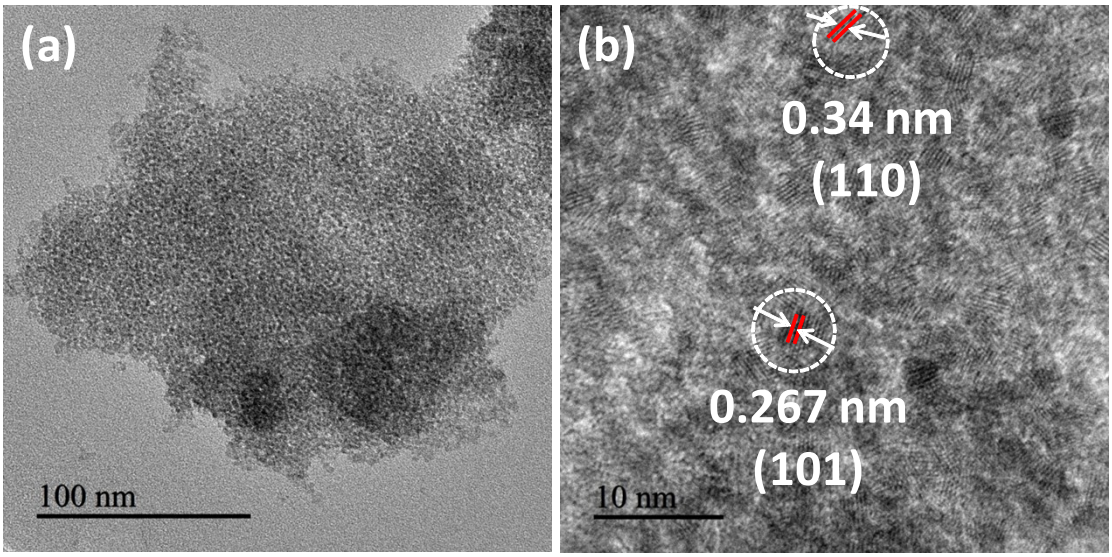

Figure S9.TEM image of SnO_2 material(a), lattice fringes (b)

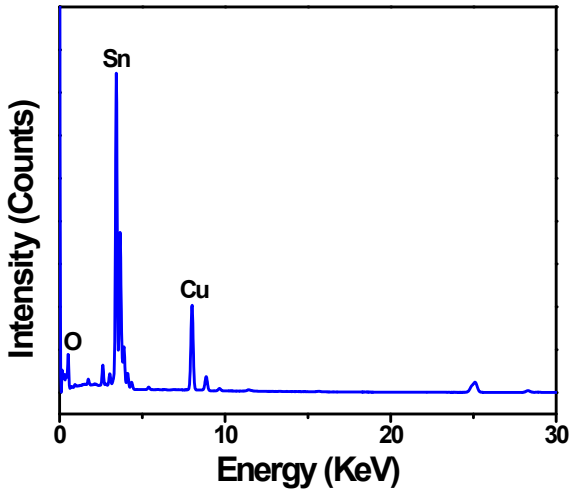

Figure S10. EDAX pattern of SnO_2 sample.

Reaction set-up:

Procedure of formation of Formic acid using mesoporous SnO_2 Photocatalyst:

The photocatalytic reduction of CO_2(1 atm) into Formic acid was performed usingonly5 mL H_2O in presence of 10 mg of SnO_2 in a 25 mL round bottom flask. The reaction was allowed to run under irradiation ofthewhite LED light at room temperature for 6 h under continuous stirring (Figure S11). At the end of the reaction, $SnO_2$was separated by filtration and the filtratewas analyzed by ^{1}H and ^{13}C NMR Spectra which confirms the formation of HCOOH. The yieldof formic acid produced was detected by using UV-Visible spectrophotometer.

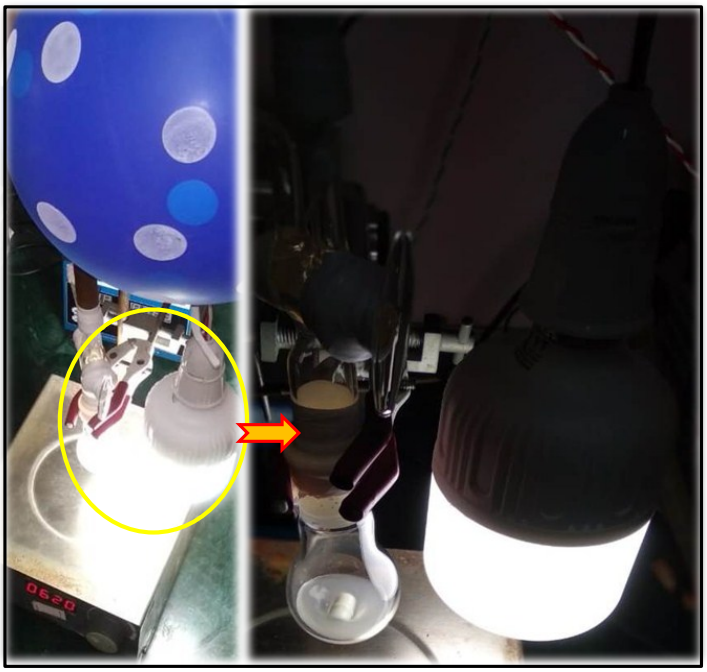

Figure S11. Photo of the photoreaction setup with CO_2 balloon directly irradiated with white LED light.

Calculation of product's yields:

Reaction yields were evaluated using calibration plot as shown Figure S12. Known concentration of HCOOH was plotted with the O.D. value in UV-vis spectra to obtain it.

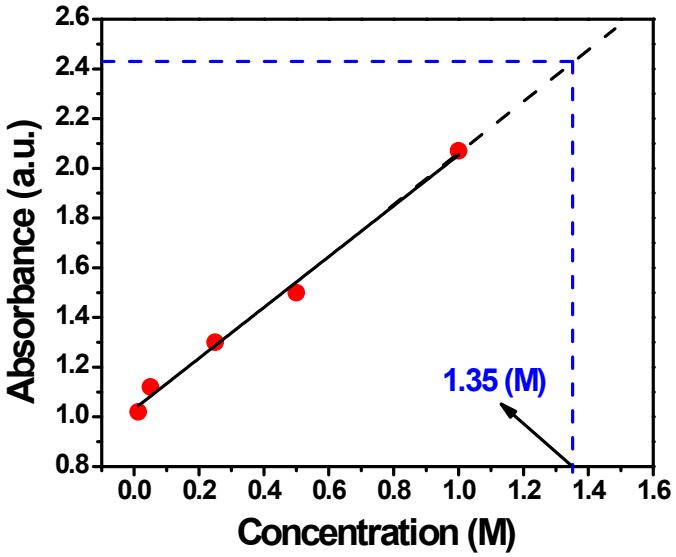

Figure S12. Calibration curve of formic acid for determination of concentration of Formic acid produced.

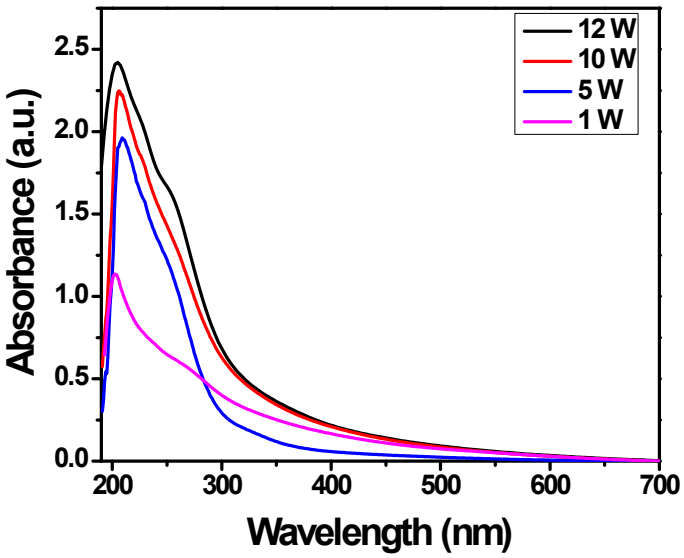

Figure S13. UV Spectra of HCOOH in H_2O for different intensities of light.

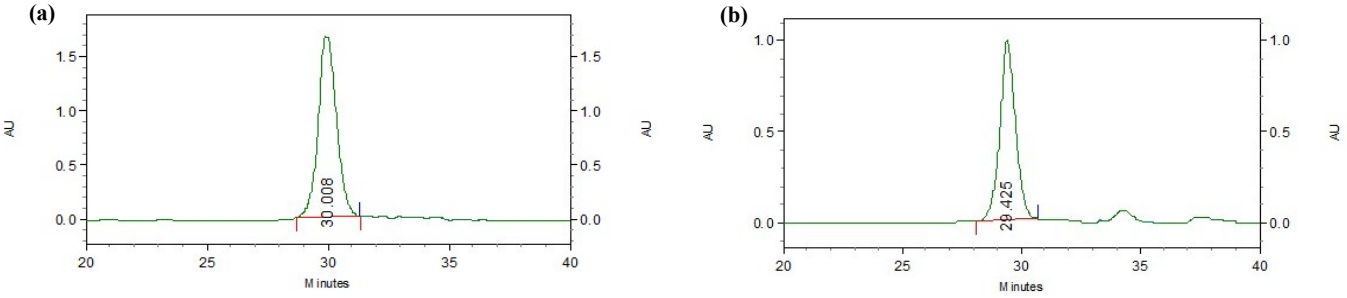

Figure S14. HPLC chromatogram for the analysis of formic acid, (a) pure 1 M formic acid as standard, (b) reaction mixture after photocatalysis**.** Column:C18, mobile phase: 5% methanol + 0.01 M KH_2PO_3 acidified to pH 2.5 via H_3PO_3, flowrate: 0.2 ml/min, injection volume: 20µl, UV wavelength: 206 nm.

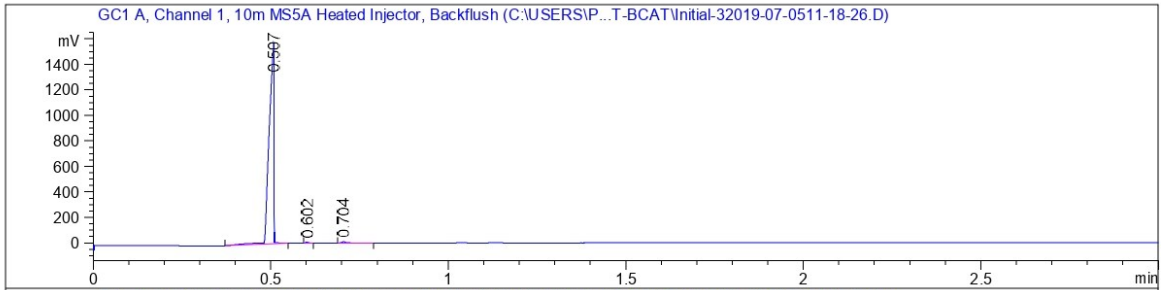

(a) CO_2 standard

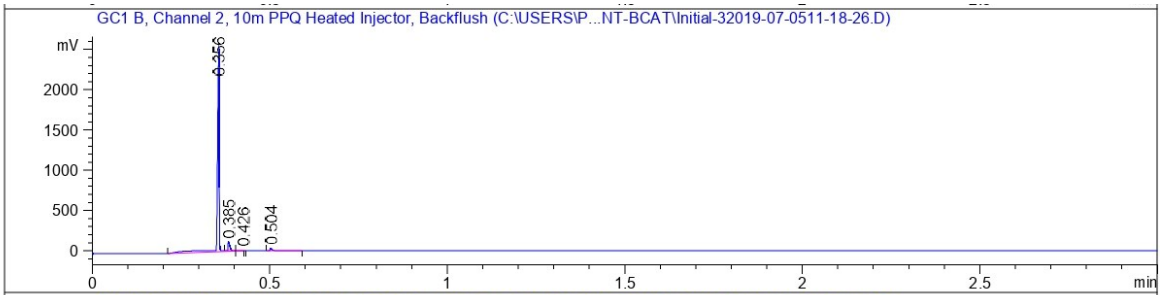

(b) H_2 standard

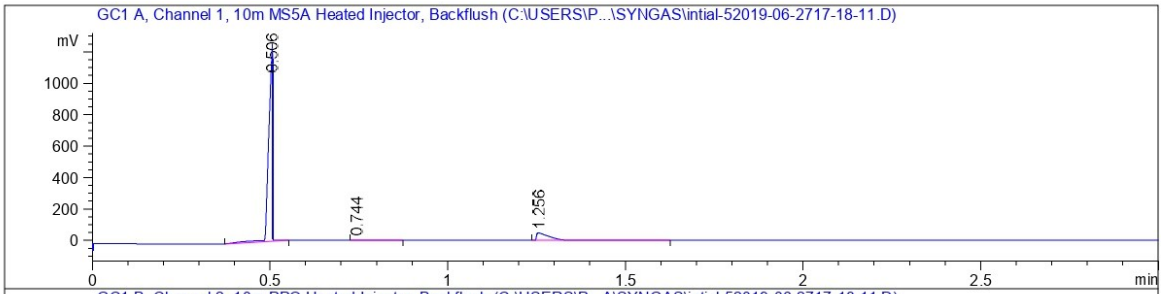

(c) Syngas Propylene(0.506 min) + CO (1.25 min)

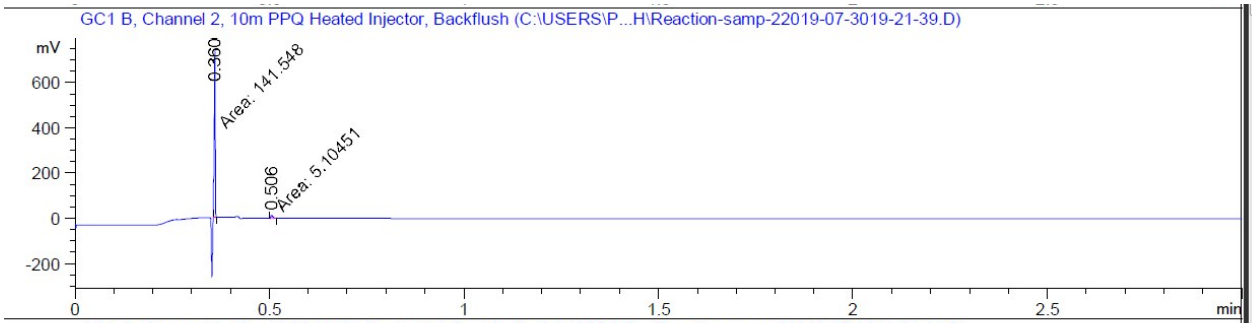

(d) Reaction mixture after photocatalysis

Figure S15. GC chromatogram (a) CO_2 standard, (b) H_2 standard, (c) Syngas Propylene(0.506 min) + CO (1.25 min), (d) Reaction mixture after photocatalysis.

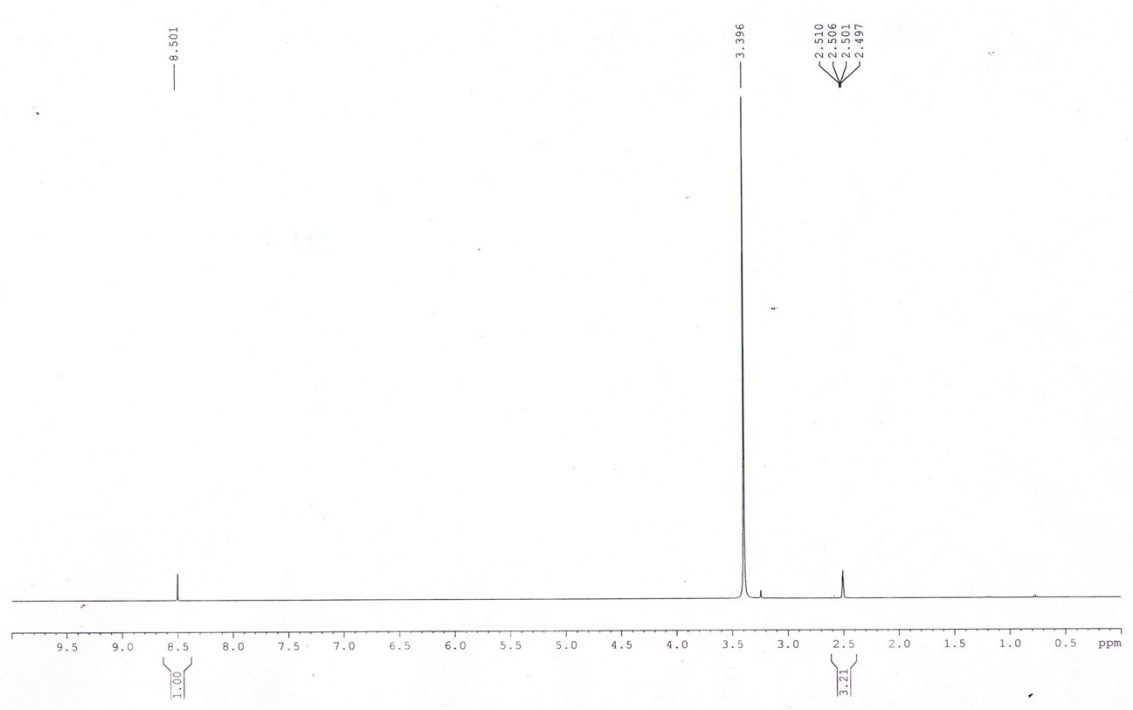

Figure S16. ^{1}H NMR spectra of formic acid

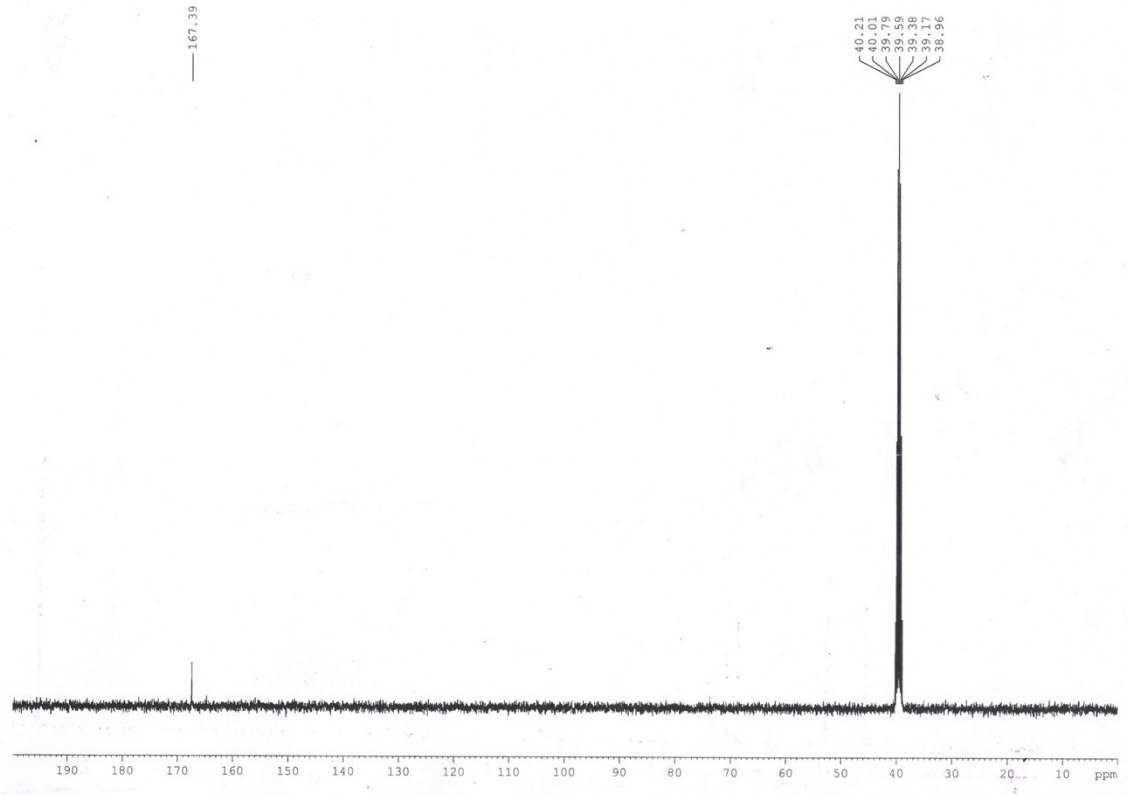

Figure S17. ^{13}C NMR spectra of formic acid

References:

[1]P. Zhang, I. Lo, D. O'Connor, S. Pehkonen, H. Cheng, D. Hou, Journal of Colloid and Interface Science, **2017**, *508*, 39-48.

[2] W. Kaewprachum, S. Wongsakulphasatch, W. Kiatkittipong, A. Striolo, C. K. Cheng, S. Assabumrungrat, Journal of Environmental Chemical Engineering, DOI:10.1016/j.jece.2019.102920.

[3] D. Chandra, N. Mukherjee, A. Mondal, and A. Bhaumik, J. Phys. Chem. C,**2008**, *112,* 8668–8674.

[4] P. S. Patil, R. K. Kawar, T. Seth, D. I. Amalnerkar, P. S. Chigare, Ceram. Int**.,2003,** *29*, 725-734.

[5] A. H. Chowdhury, P.Bhanja, N. Salam, A.Bhaumik, S. M. Islam, Molecular Catalysis,**2018**, *450*, 46–54.

[6] Q. Zhao, D. Ju, X. Deng, J. Huang, B. Cao, X. Xu, Scientific Reports, **2015**, *5*,7874.

[7] B. Cheng, J. M. Russell, W. Shi, L. Zhang, and E. T. Samulski, J. AM. CHEM. SOC. **2004**, *126*, 5972-5973.

[8] J. Senthilnathan, L. Philip, Chemical Engineering Journal, **2010**,*161,*83–92.